Impact adding bifurcation in an autonomous hybrid dynamical model of church bell

P. Brzeski[a], A.S.E. Chong[b], M. Wiercigroch[c], P. Perlikowski[a]

[a] *Division of Dynamics, Technical University of Lodz, Stefanowskiego 1/15, 90-924 Lodz, Poland*
[b] *Facultad de Ciencias Naturales y Matemàticas, Escuela Superior Politécnica del Litoral, P.O. Box 09-01-5863, Guayaquil, Ecuador*
[c] *Centre for Applied Dynamics Research, School of Engineering, University of Aberdeen, Kings College Aberdeen AB24 3UE, Scotland, UK*

Abstract

In this paper we present the bifurcation analysis of the yoke-bell-clapper system which corresponds to the biggest bell "Serce Lodzi" mounted in the Cathedral Basilica of St Stanislaus Kostka, Lodz, Poland. The mathematical model of the system considered in this work has been derived and verified based on measurements of dynamics of the real bell. We perform numerical analysis both by direct numerical integration and path-following method using toolbox ABESPOL ([4]). By introducing the active yoke the position of the bell-clapper system with respect to the yoke axis of rotation can be easily changed and it can be used to probe the system dynamics. We found a wide variety of periodic and non-periodic solutions, and examined the ranges of coexistence of solutions and transitions between them via different types of bifurcations. Finally, a new type of bifurcation induced by a grazing event - an "impact adding bifurcation" has been proposed. When it occurs, the number of impacts between the bell and the clapper is increasing while the period of the system's motion stays the same.

Keywords: Bells, nonlinear dynamics, impacts, hybrid system, bifurcation analysis, impact adding bifurcation

1. Introduction

Bells have been musical and ceremonial instruments with a very long history and well established role in a culture. They were invented in China and have been used all around the world [8]. Today, their sound announces and upgrades significance of major events. Depending on the region bells are mounted in a number of different ways basing on local customs and tradition. In Europe we have three different characteristic mounting layouts: Central European, English and Spanish [9]. In Central Europe, bells usually tilt on their axis with maximum amplitude of oscillations below 90 degrees. In the English, system the amplitude of oscillations is greater and bells perform nearly a complete rotations in both directions. Conversely, in the Spanish system bells rotate continuously in the same direction. All these mounting layouts were developed throughout centuries based on experience and intuition of bell-founders and craftsmen. It is common that the bells are casted using casting moulds passed down from father to son and so forth. Although the design of a bell, its yoke, clapper and a belfry has been being improved over the years, their modelling and dynamical analysis is still a challenging task.

The dynamics a yoke-bell-clapper system is complex and difficult to analyze due to its nonlinear characteristics, repetitive impacts and piecewise smooth nature of its excitation. In 19th century Wilhelm Veltmann made a a first

attempt to describe mathematically the behaviour of the famous Emperor's Bell in the Cologne Cathedral [27, 28] by using a double pendulum to model the bell and the clapper. Heyman and Threlfrall [10] used a similar model to estimate inertia forces induced by a swinging bell. The impoartant issue during yoke design is the knowledge of loads created by ringing bells. This can significantly improve the overall dynamics and reliability of the system [23, 15, 1]. The analysis of bells' sound is always performed via Finite Elements Methods [24, 12, 7], while in modelling of their dynamics, there is a tendency to use much simpler hybrid dynamical models of the yoke-bell-clapper system, e.g.[16]. This model has been improved in our recent paper [19] based on the experimental studies where parameters' values were determined from the measurements of the biggest bell in the Cathedral Basilica of St Stanislaus Kostka, Lodz, Poland. Then, in [20] we focused on the description of different ringing schemes and their coexistence of stable solutions. In the very recent work [3], we show the method to prepare the model of the yoke-bell-clapper system with external excitation for continuation in ABESPOL toolbox [4] and we show the bifurcation diagram for varying excitation's torque.

In this paper, we present the bifurcation analysis taking the yoke geometry as a bifurcation parameter. Let us first briefly discuss possible scenarios of stabilization and destabilization of periodic solutions in the context of non-smooth dynamics, which has witnessed a rapid development recently. The bifurcation theory of smooth systems is mature and we know all bifurcations with co-dimension 1 and 2 [32, 13]. In the smooth systems we can distinguish the following typical local bifurcations: period doubling, Neimark-Sacker, pitchfork and saddle-node. The first three bifurcations cause destabilisation of the current periodic solution and emergence of new a periodic solution with different features. The exception is the saddle-node bifurcation, which takes place when stable and usable orbits collide and annihilate each other. In the non-smooth systems, we observe all aforementioned bifurcations and additionally grazing, period adding, corner and sliding bifurcations [2, 6, 18, 21, 25, 14]. Nevertheless, we still do not have a full catalogue of non-smooth bifurcations. In our investigations, we have focused on the grazing bifurcation [31, 22, 29, 11] and grazing induced bifurcations [17, 30]. Grazing bifurcations may induce different events such as: a sudden loss of stability or existence of the orbit, a creation of new periodic orbit or multiple orbits, a change in the period of the system's motion or creation of a chaotic attractor. Most of known non-smooth bifurcations heve been detected in the simple systems, where one can perform analytical investigations. However, there is a large group of complex systems which cannot be analysed analytically and for which one can expect new non-smooth bifurcations. The main reason for that is the lack of easy, accessible tools to analyse the complex non-smooth systems via path-following. Recently, new path-following toolboxes TC-Hat [26], Coco [5] and ABESPOL [4] have been developed. Thanks to such software the analysis of non-smooth systems is now possible even in complex cases like yoke-bell-clapper system, where we have multiple nonlinearities.

In this paper, we consider the application of the active yoke which let us change the position of the bell-clapper system in respect to the axis of rotation of the yoke. We show its influence on the dynamical response of the system and present the existence of several periodic and non-periodic solutions, the ranges of coexistence of solutions and

transitions between them via different bifurcation scenarios. Finally, we introduce a new kind of bifurcation induced by a grazing event - an "impact adding bifurcation".

The paper is organized as follows. In Section 2 we describe the hybrid dynamical model of the church bell and introduce the active yoke. The results of the path-following are shown in Section 3. In Section 4 the conclusions are drawn.

2. Physical and mathematical models

The hybrid dynamical model of the yoke-bell-clapper system considered in this paper has been described in detail in our previous publication [19]. To calibrate the model and determine its parameters we have performed detailed measurements of the bell named The Heart of Lodz (the biggest bell in the Cathedral Basilica of St Stanislaus Kostka in Lodz). The model was then tuned and validated by comparing the results of numerical simulations with the data collected during a series of experiments proving to be a reliable predictive tool and capable to simulate the behaviour of a parameters. The next subsections briefly describe the model and present the influencing parameters.

2.1. Geometry of the yoke-bell-clapper system

The developed mathematical model is based on the analogy between freely swinging bell and the motion of the equivalent double physical pendulum. The first pendulum has fixed axis of rotation and models the yoke together with the bell that is mounted on it. The second pendulum is attached to the first one and imitates the clapper. Figs 2.1 (a,b) show schematics indicating the position of the rotation axes of the bell o_1, the clapper o_2 and presenting parameters involved in the model. For the sake of simplicity, henceforth, the term "bell" is used for the bell and its yoke, which is treated as one solid element.

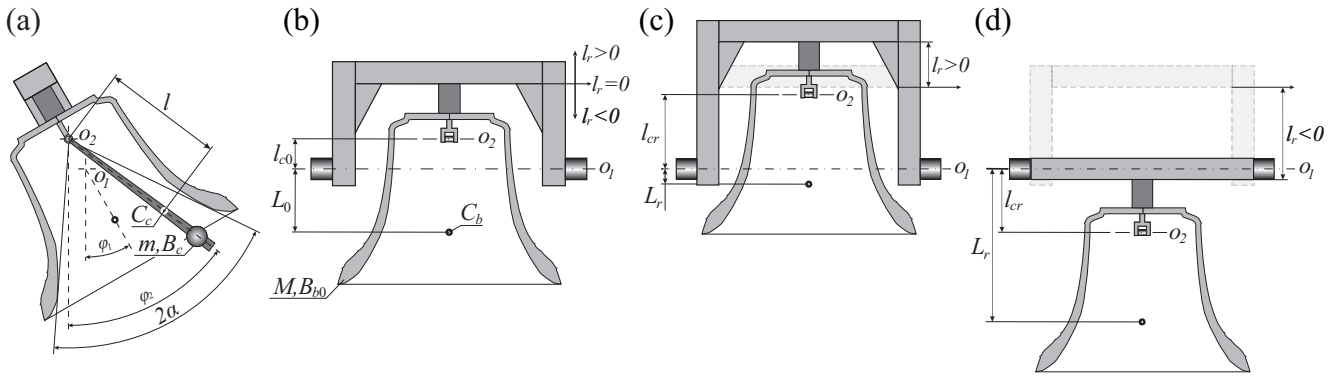

Figure 2.1: Schematics of the physical model in different planes to show its geometry and kinematics.

The model has eight physical parameters: L_0 describes the distance between the rotation axis of the bell and its centre of gravity (point C_b), l is the distance between the rotation axis of the clapper and its centre of gravity (point C_c). The distance between the bell's and the clapper's axes of rotation is given by l_{c0}. The mass of the bell

is described by M, while B_{b0} characterizes the bell's moment of inertia referred to its axis of rotation. Similarly, m describes the mass of the clapper and B_c stands for the clapper's moment of inertia referred to its axis of rotation. Parameter l_r is used to describe the modifications of the yoke, as it is presented in Fig. 2.1(b-c). The l_r definition is explained in detail in our previous paper [20], where $l_r = 0$ refers to the shape of original yoke used in the Cathedral's bell. If the centre bell's of gravity is lowered with respect to its axis of rotation, $l_r < 0$, otherwise $l_r > 0$. The change of the yoke design given by the value of l_r affects other parameters. Therefore, in the mathematical model, the following parameters that describes the system with the modified yoke are used:

$$L = L_0 - l_r, \qquad l_c = l_{c0} - l_r, \qquad B_b = \left(B_{b0} - ML_0^2\right) + ML^2. \tag{2.1}$$

A planar co-ordinate system is used as shown in Fig.2.1 (a), where the angle between the bell's axis and the downward vertical is given by φ_1 and the angle between the clapper's axis and downward vertical by φ_2. Angular parameter α describes the impact condition as follows:

$$|\varphi_1 - \varphi_2| = \alpha. \tag{2.2}$$

Synonymously, contact between the bell and the clapper occurs when a relative angular displacement between the bell and the clapper is equal to α.

2.2. Mathematical model

In this section the mathematical model used to simulate dynamic responses of the investigated yoke-bell-clapper system is presented. Lagrange equations of the second type are employed to derive two coupled second order ODEs that describe the motion of the considered system (the full derivation can be found in [19]):

$$\left(B_b + ml_c^2\right)\ddot{\varphi}_1 + ml_c l\ddot{\varphi}_2\cos\left(\varphi_2 - \varphi_1\right) - ml_c l\dot{\varphi}_2^2\sin\left(\varphi_2 - \varphi_1\right) + \left(ML + ml_c\right)g\sin\varphi_1 + D_b\dot{\varphi}_1 - D_c\left(\dot{\varphi}_2 - \dot{\varphi}_1\right) = T(\varphi_1), \tag{2.3}$$

$$B_c\ddot{\varphi}_2 + ml_c l\ddot{\varphi}_1\cos\left(\varphi_2 - \varphi_1\right) + ml_c l\dot{\varphi}_1^2\sin\left(\varphi_2 - \varphi_1\right) + mgl\sin\varphi_2 + D_c\left(\dot{\varphi}_2 - \dot{\varphi}_1\right) = 0, \tag{2.4}$$

where g stands for gravity and $T(\varphi_1)$ describes the effects of the linear motor propulsion. The motor excites the bell - when its deflection from vertical position is smaller than $\pi/15\,[rad]$ (12^o). The torque generated by the motor $T(\varphi_1)$ is given by the piecewise formula:

$$T(\varphi_1) = \begin{cases} T_{max}\,\mathrm{sgn}(\dot{\varphi}_1)\,\cos\left(7.5\varphi_1\right), & if \quad |\varphi_1| \leq \frac{\pi}{15} \\ \\ 0, & if \quad |\varphi_1| > \frac{\pi}{15} \end{cases} \tag{2.5}$$

where T_{max} is the maximum torque. Although, the above expression is not fully accurate reflection of the effects generated by the linear motor it is able to reproduce the characteristics of the modern bells' driving mechanisms [19].

We use a discreet impact model. If Eq. 2.2 is fulfilled, the numerical integration process is paused. Then, simulation is restarted with updated initial conditions. The bell's and the clapper's angular velocities are swaped from the values before the impact to the ones after the impact. The angular velocities after the impact are obtained by taking into account the energy dissipation and the conservation of the system's angular momentum that are expressed by the following formulas:

$$\frac{1}{2}B_c\left(\dot{\varphi}_{2,AI}-\dot{\varphi}_{1,AI}\right)^2 = k\frac{1}{2}B_c\left(\dot{\varphi}_{2,BI}-\dot{\varphi}_{1,BI}\right)^2, \tag{2.6}$$

$$\begin{aligned}\left[B_b+ml_c^2+ml_cl\cos\left(\varphi_2-\varphi_1\right)\right]\dot{\varphi}_{1,BI}+\left[B_c+ml_cl\cos\left(\varphi_2-\varphi_1\right)\right]\dot{\varphi}_{2,BI} = \\ \left[B_b+ml_c^2+ml_cl\cos\left(\varphi_2-\varphi_1\right)\right]\dot{\varphi}_{1,AI}+\left[B_c+ml_cl\cos\left(\varphi_2-\varphi_1\right)\right]\dot{\varphi}_{2,AI}\end{aligned} \tag{2.7}$$

where index AI stands for "after impact", index BI for "before impact" and parameter k is the coefficient of energy restitution and in our simulations we assume $k = 0.05\,[-]$ [19].

The mathematical model contains eleven parameters that have the following values: $M = 2633\,[kg]$, $m = 57.4\,[kg]$, $B_b = 1375\,[kgm^2]$, $B_c = 45.15\,[kgm^2]$, $L = 0.236\,[m]$, $l = 0.739\,[m]$, $l_c = -0.1\,[m]$ and $\alpha = 30.65^o = 0.5349\,[rad]$, $D_c = 4.539\,[Nms]$, $D_b = 26.68\,[Nms]$, $T_{max} = 230\,[Nm]$. Eqs 2.3 and 2.4 together with the impact model create a hybrid dynamical system.

3. Bifurcation analysis of periodic orbits

In this Section typical bifurcation scenarios for transitions between different periodic solutions are presented. As mentioned in the description of system parameters, in practice, only the design of the yoke and driving mechanism can be altered. These changes are decsribed by l_r and T_{max}. In [20] we investigated the influence of these parameters and developed ringing scheme diagrams that show which working regime will be achieved for different l_r and T_{max} values (starting from zero initial conditions). Using direct numerical integration the ranges of parameters values that ensure that the required type of behaviour will be reached when starting from equilibrium state are identified. In [3] we presented the path-following analysis of periodic solutions, where the amplitude of driving force T_{max} is a bifurcation parameter assuming constant geometry of yoke.

In this article, the influence of the geometrical parameter l_r describing the yoke design is investigated. Our analysis reveals a rich bifurcation scenarios leading to and emerging from periodic orbits of different type. We analyse stable and unstable responses, and show transitions between different periodic regimes. The undertaken analysis is performed by both a direct numerical integration and a path-following methods. The path-following

analysis was carried out with ABESPOL toolbox based on Coco [4]. The implementation of the hybrid model for continuation in ABESPOL was a challenging task and required a lot of effort. Process of implementation is described in detail in our previous paper [3], where we present operation modes and discontinuity events that we use when running continuation.

In Fig. 3.1 two bifurcation diagrams are shown with the bifurcation parameter (l_r) on the horizontal axis and on the vertical one the angular position of the clapper (φ_2) recorded when $\varphi_1 = 0$ and $\dot{\varphi}_1 > 0$. The results presented in panel (a) are obtained by a direct numerical integration while ones on panel (b) by path-following method. Panel (a) gives an overview of stable solutions as this figure is obtained by merging four bifurcation diagrams that are depicted with different colours. Green dots correspond to computation from $l_r = -0.3\,[m]$ to $l_r = 0.2\,[m]$, purple dots have been obtained by integration in reverse direction. In addition blue and yellow dots are the result of two additional trials, each starting from different initial conditions.

The results obtained using direct numerical integration were used as initial guesses for path-following analysis, which results were obtained by ABESPOL and are shown in Fig. 3.1 (b). A continuation enables to detect bifurcation points, determine their type and investigate evolution of unstable orbits. However in this study, only solutions that have a known physical meaning are considered, hence unstable branches born at grazing bifurcations were disregarded. Eleven different periodic solutions were detected, whcih are marked with a different colour and given a number.

For low values of geometrical parameter $l_r \epsilon\, (-0.3,\, -0.2522)\ [m]$, we observe a non-impacting solution marked as (1) and shown with a black solid line. In that range, the yoke geometry is such that the clapper cannot reach the bell shell and there is no contact. This solution remains stable with the increase of l_r until the grazing-induced bifurcation occuring at $l_r = -0.252\,[m]$ (vertical line in Fig. 3.1). In that point, the non-impacting solution loses its stability and six different unstable solutions (2, 3, 4, 6, 7, 8) are born.

In Fig. 3.2 a zoom-up of the bifurcation diagram around that grazing-induced bifurcation point ($l_r = -0.252[m]$) is presented. In the plot one can see six unstable branches that meet in the bifurcation point. Solution (2) is a period-5 symmetric solution with two impacts. This means that for five periods of bell's oscillations, which is one full period of this solution, two impacts (one on each side of the bell) are observed. This solution is initially unstable but stabilizes through a saddle-node bifurcation ($l_r = -0.2522\,[m]$) and remains stable until grazing point at $l_r = -0.2446[m]$. Solutions (3) and (4) are both asymmetric with one impact per two periods of bell's oscillations. These solutions stabilize at a period doubling bifurcations at $l_r = -0.2403\,[m]$ and destabilize in grazing points at $l_r = -0.2186\,[m]$. Because of the asymmetry, the destabilization occurs at grazing on the right hand boundary for solution (3) and on the left hand boundary for solution (4). Solutions 6, 7, 8 are also born in this bifurcation but their ranges of existence is much wider.

In Fig. 3.1(a) we observe the large range ($l_r \in \langle -0.2446,\, 0.1473\rangle\ [m]$) of non-periodic behaviour for which the bell and the clapper collide in a chaotic manner. Within the chaotic range a window with period-3 symmetric

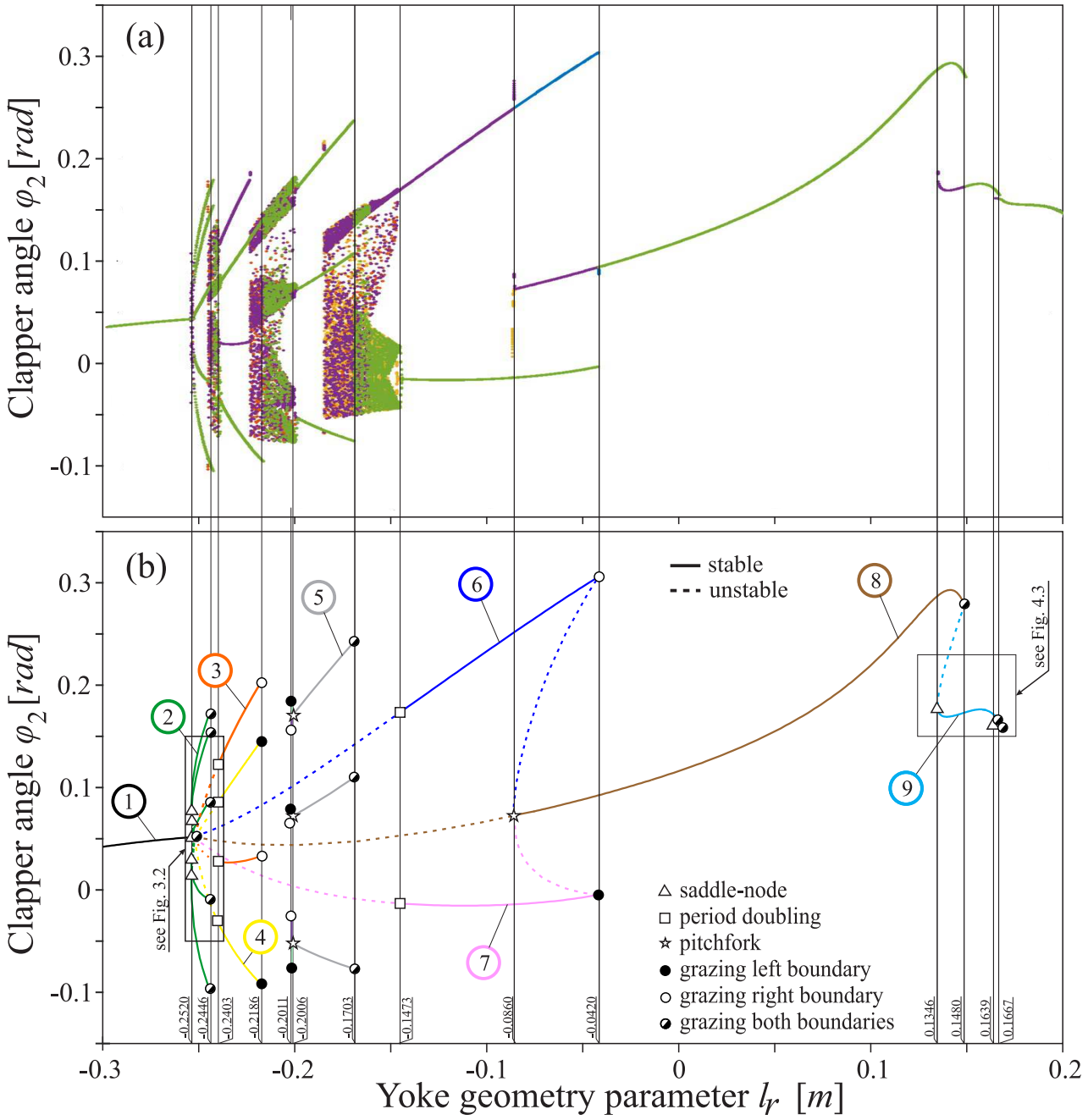

Figure 3.1: Bifurcation diagrams of the clapper angle φ_2 as a function of yoke geometry parameter l_r. Results were obtained by a direct numerical integration (a) and path-following (b) for fixed amplitude of excitation $T_{max} = 230\,[Nm]$ and $l_r \in \langle -0.3,\, 0.2\rangle\ [m]$. Different types of solutions are marked with different numbers and colours. Solid curves mark stable solutions, where dashed ones unstable parts of branches. Symbols are used to distinguish different bifurcations (see legend). Vertical lines mark the position of bifurcation points in which the stability changes.

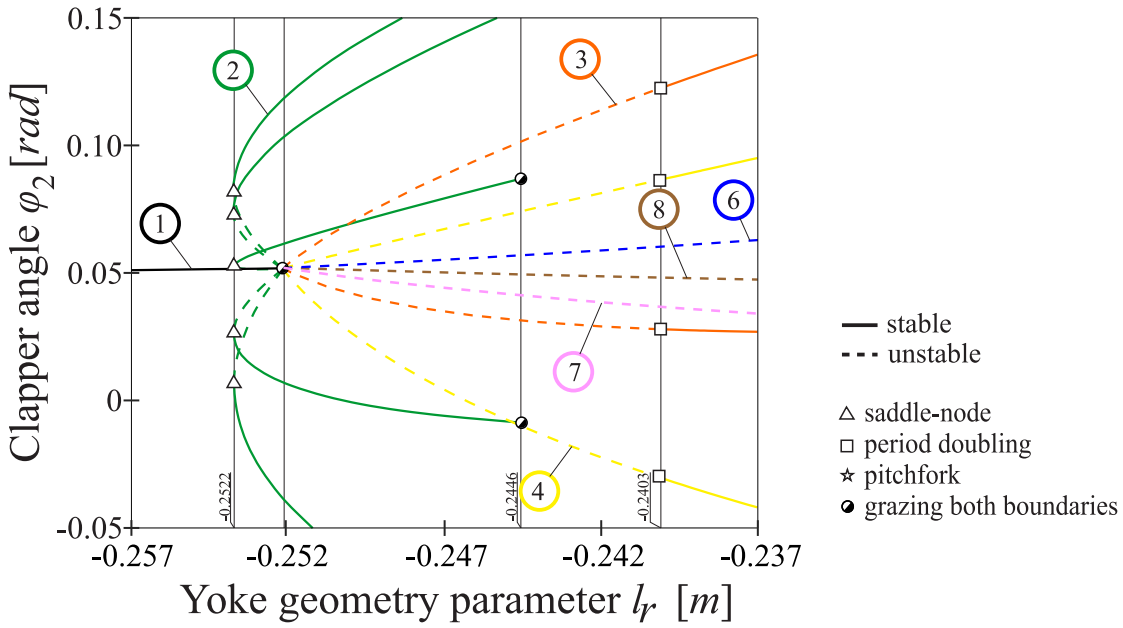

Figure 3.2: Zoom-up of bifurcation diagram shown in Fig. 3.1 that shows in details subcritical pitchfork bifurcation that occurs for $l_r = -0.252\,[m]$. Different types of solutions are marked with different numbers and colours. Solid curves mark stable solutions, where dashed ones unstable parts of branches. Symbols are used to distinguish different bifurcations (see legend).

solution (5) with two impacts (one on each side of the bell) was found. This solution is stable in the range $l_r \in \langle -0.2006,\, 0.1703\rangle\ [m]$. For $l_r = -0.1703\,[m]$ its destabilization occurs at a grazing event (simultaneously on both boundaries) while for $l_r = -0.2006\,[m]$ supercritical pitchfork bifurcation occurs - specifically a symmetry breaking bifurcation. In that point two new asymmetric solutions are born. These solutions are stable in a very narrow range $l_r \in \langle -0.2011,\, -0.2006\rangle\ [m]$ (for $l_r = -0.2011\,[m]$ grazing occurs).

After the chaotic range two stable asymmetric solutions (6) and (7) can be observed. These are asymmetric attractors with period-1 and one impact per period (on the right hand boundary for solution (6), and on the left hand boundary for solution (7)). Branches (6) and (7) are created at a grazing induced bifurcation that occurs for $l_r = -0.252\,[m]$ (see Fig. 3.2). Initially, both solutions (6) and (7) are unstable. With the increase of l_r value a period doubling bifurcation occurs for $l_r = -0.1473\,[m]$. After this point solutions (6) and (7) become stable and remain such until the grazing point is reached at $l_r = -0.042\,[m]$.

The last branch that is created in the grazing event at $l_r = -0.252\,[m]$) corresponds to solution (8). It is a symmetric period-1 attractor with two impacts per period (one at each side). Such behaviour is commonly encountered in practice and often called symmetric falling clapper. Initially, solution (8) is unstable until subcritical pitchfork bifurcation (symmetry breaking) that occurs at $l_r = -0.086\,[m]$. After this point, solution (8) remains stable up to $l_r = 0.148\,[m]$ for which it is destabilized via grazing on both boundaries. This solution is stable in a particularly wide range of $l_r \in \langle -0.086,\, 0.148\rangle\ [m]$. It is of practical importance and indicates that this solution can be fairly easily achieved using different yoke designs (different geometry). Moreover, for $l_r \in \langle -0.086,\, -0.042\rangle\ [m]$ a range where symmetric (8) and asymmetric (6,7) solutions co-exist is observed. Therefore, it is possible to design

the yoke so that the bell can work in two different regimens. In such case, different solutions can be reached by applying, for example, different starting procedures.

3.1. Impact adding bifurcation

Grazing bifurcation that is observed for $l_r = 0.148\,[m]$ creates a solution (9) (see Fig. 3.1). It is a period-1 attractor with four consecutive impacts - on each side of the bell's shell two impacts occur immediately one after another. Such behaviour is called "double kiss". Initially solution (9) is unstable. It stabilizes at a saddle-node point ($l_r = 0.1346\,[m]$). When further increasing l_r similar bifurcation scenario occurs. This sequence of recurrent grazing events and saddle-node bifurcations is shown in detail in Fig. 3.3. Firstly, one can see a grazing event in which period-1 solution (10) is created with six consecutive impacts - on each side of the bell three impacts occur immediately one after another. This means, that on each side we have one more impact then in solution (9). Similarly to solution (9) also solution (10) is initially unstable and stabilizes at a saddle-node bifurcation. Then, with the increase of l_r value, similar bifurcation sequence is repeated. Solution (11) with eight impacts is created (four on each side) and stabilized in a saddle-node bifurcatoin. It is important to notice, that in the above described bifurcation scenario we do not observe any changes of the overall period of attractors (the period increases only due to the increase of length l_r). This means that each new attractor created in an "impact adding bifurcation" contains more impacts has the same period.

Phenomenon described above is repeatable and results in a sequence of recurrent changes in attractors. Although the change in the phase portrait of an attractor is minor (see Fig. 3.4) these solutions can be easily distinguished by listeners because of different number of impacts. Up to our knowledge, such scenario of recurrent bifurcations has not been described yet. Still, it is characteristic for hybrid dynamical systems similar to the one investigated in the paper. Due to the type of attractor changes we name this grazing event as "impact adding bifurcation".

The far right part of the bifurcation diagram obtained by integration is the sliding motion (Fig. 3.1(a)). It cannot be analysed using the path-following method because the major part of this solution is the stick phase (the bell and the clapper are in continuous contact). In our continuation toolbox such behaviour would be considered as a series of impacts and infinite number of segments should be introduced to replicate the sticking of the bell and the clapper. Alternatively, the condition for sticking and the new segment for continuation could be defined to sove this problem. Still, this would make our model surjective and impede the analysis. Hence, we present only the results from direct numerical integration.

3.2. Phase portraits of the analysed solutions

Fig. 3.4 presents the phase portraits for all eleven solutions analysed in the paper. For each solution there are two panels (a) and (b) named with its number. Panels (a) present phase portraits with the angular displacement of the clapper (φ_2) versus the displacement of the bell (φ_1), while panels (b) present phase portraits of the clapper itself (velocity ($\dot{\varphi}_2$) versus displacement (φ_2)). The gaps in panels (b) emerge as an outcome of the hybrid nature of the dynamical model. To mark the impact conditions, on each panel (a) we plot two straight lines between which

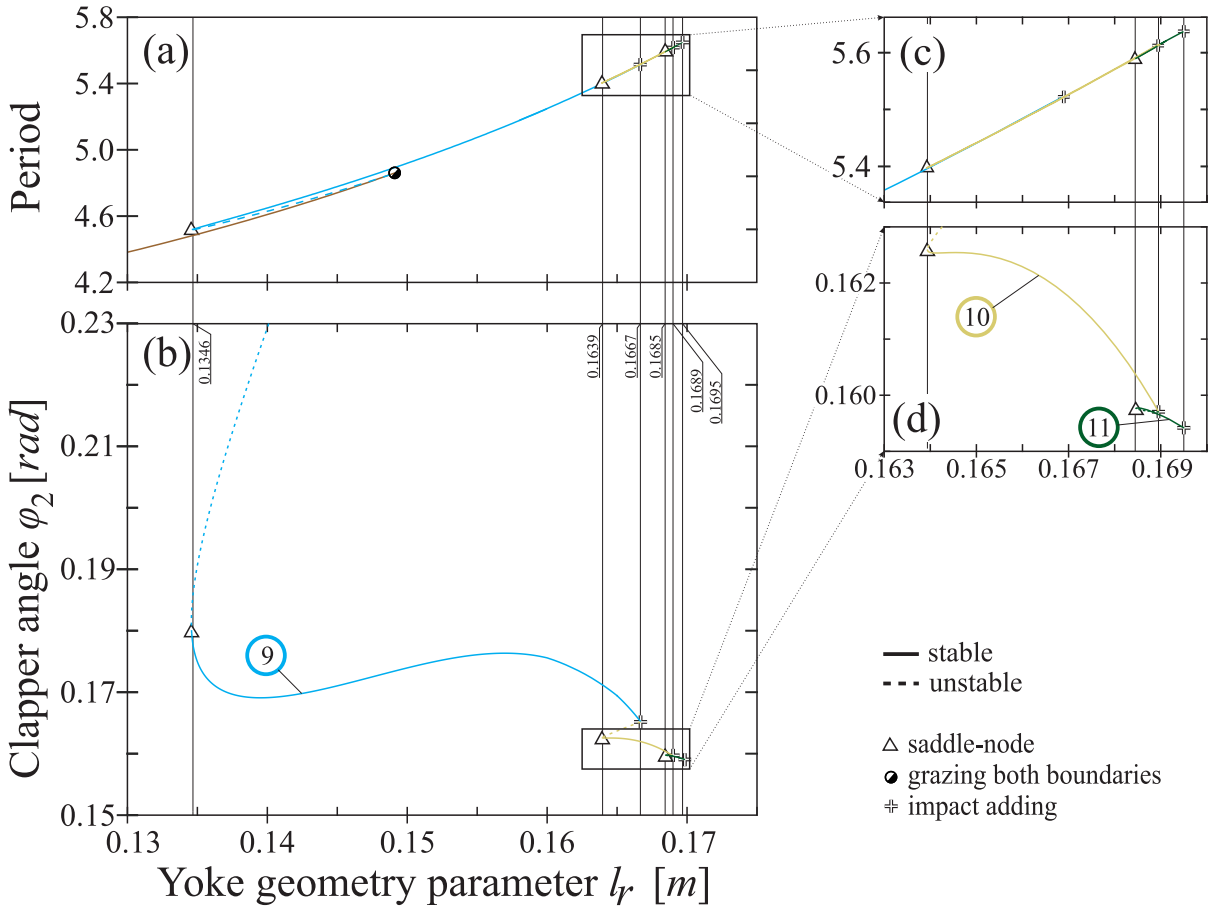

Figure 3.3: Zoom-ups of of bifurcation diagram shown in Fig. 3.1. Panel (b) shows in details sequence of period adding bifurcations that is magnified in panel (d). Panels (a) and (c) show the changes in the overall period of attractors. Different types of solutions are marked with different numbers and colours. Solid curves mark stable solutions, while dashed ones unstable parts of branches. Symbols are used to distinguish different bifurcations (see legend). Vertical lines mark the position of bifurcation points in which the stability changes.

the phase portrait exists. Impact occurs when the trajectory reaches one of the impact condition lines. For a better understanding of these figures, as the reference we will now describe the solution from branch (8) shown in panels 8(a,b). It is an attractor with two impacts per one period of motion. By analysing panels 8 (a,b) we see that the attractor is symmetric with respect to the origin of the coordinate system. Hence, we observe identical collisions on both sides of the bell. On panel 8(b) we observe two jumps in the trajectory trace that refer to impacts - one at each side of the bell, also in panel 8(a) we see that the trajectory touches both lines, hence the impact condition is fullfilled two times.

4. Conclusions

Bells are simple musical instruments which exhibit rich variety of dynamical behaviours. Ringing scheme depends basically on the design of the yoke and propulsion which usually follow local traditions. Still, to design the yoke one needs to analyze the dynamics of the yoke-bell-clapper system and determine the ranges of parameters with single solution. In the paper, we focus on the influence of the yoke geometry described by parameter l_r. Results from both direct numerical integration and the path-following method are presented. The path-following analysis reveals unstable solutions and enables to detect the bifurcations that occur along them.

From the mathematical point of view the investigated model is nonlinear, non-smooth and piecewise smooth, hence it has complex dynamics. An important feature of the investigated system is its specific piecewise forcing that ensures that the bell always oscillates with its natural frequency.

Complete bifurcation sequences, which are characteristic for hybrid dynamical systems are presented and discussed. Typical bifurcations including grazing, saddle-node, pitchfork and period doubling bifurcations were detected. The ranges of stability for each solution were defined with a detailed explanation of how the stability changes.

The main finding from the study is a new kind of bifurcation induced by a grazing event - an “impact adding bifurcation”. When “impact adding bifurcation" occurs, the number of impacts increases while the period attractor persists the same. It is a new type of phenomenon that persists in the investigated model. Similar bifurcation scenarios can occur in a wide range of hybrid systems, especially for ones with similar forcing similar to the one investigated in this work.

Acknowledgement

This study was supported by Lodz University of Technology (K113/9117DS). PB is supported by the Foundation for Polish Science (FNP).

References

[1] D. Bettge , C-P Bork. Failures of berlin freedom bell since 1966. *Engineering Failure Analysis*, 43:63–76, 2014.

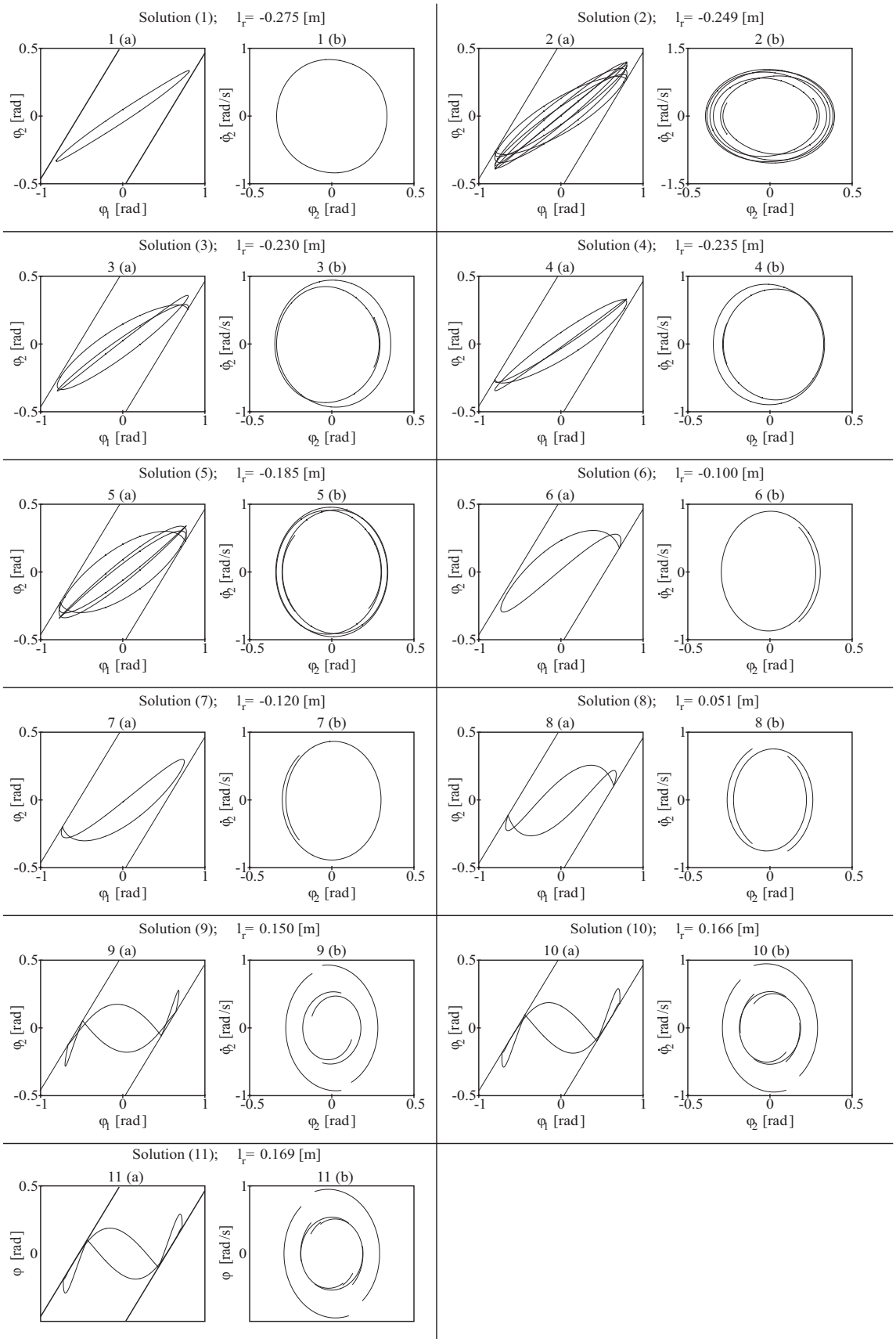

Figure 3.4: Phase portraits of the displacements of the bell and the clapper (panels (a)) and displacement versus velocity of the clapper (panels (b)). Numbers of solutions correspond to the number of branches of stable periodic attractors marked in Figs 3.1, 3.2 and 3.3.

[2] W. Chin, E. Ott, H. E Nusse, C. Grebogi. Universal behavior of impact oscillators near grazing incidence. *Physics Letters A*, 201(2-3):197–204, 1995.

[3] A. S. E. Chong, P. Brzeski, M. Wiercigroch, and P. Perlikowski. Path-following bifurcation analysis of church bell dynamics. *Journal of Computational and Nonlinear Dynamics* 12(6), 061017, 2017.

[4] A.S.E. Chong. *Numerical modelling and stability analysis of non-smooth dynamical systems via ABESPOL.* PhD thesis, University of Aberdeen, 2016.

[5] H. Dankowicz and F. Schilder. *Recipes for Continuation.* Society for Industrial and Applied Mathematics, Philadelphia, PA, 2013.

[6] M. Di Bernardo, C.J. Budd, A.R. Champneys. Corner collision implies border-collision bifurcation. *Physica D: Nonlinear Phenomena*, 154(3):171–194, 2001.

[7] A. Golas, R. Filipek. Digital synthesis of sound generated by tibetan bowls and bells. *Archives of Acoustics*, 41(1):139–150, 2016.

[8] H. Huang. Prehistoric music culture of china. *Cultural Relics of Central China*, (3):18–27, 2002.

[9] S. Ivorra, M. Palomo, G. Verdú, A. Zasso. Dynamic forces produced by swinging bells. *Meccanica*, 41(1):47–62, 2006.

[10] B.D. Threlfall, J. Heyman. Inertia forces due to bell-ringing. *International Journal of Mechanical Sciences*, 18:161–164, 1976.

[11] M. Wiercigroch J. Ing, E. Pavlovskaia. Dynamics of a nearly symmetrical piecewise linear oscillator close to grazing incidence: Modelling and experimental verification. *Nonlinear Dynamics*, 46(3):225–238, 2006.

[12] J. Klemenc, A. Rupp, M. Fajdiga. Dynamics of a clapper-to-bell impact. *International Journal of Impact Engineering*, 44:29–39, 2012.

[13] Y.A. Kuznetsov. *Elements of applied bifurcation theory*, volume 112. Springer Science & Business Media, 2013.

[14] R. Leine, H. Nijmeijer. *Dynamics and bifurcations of non-smooth mechanical systems*, volume 18. Springer Science & Business Media, 2013.

[15] D. Foti M. Lepidi, V. Gattulli. Swinging-bell resonances and their cancellation identified by dynamical testing in a modern bell tower. *Engineering Structures*, 31(7):1486 – 1500, 2009.

[16] G. Meneghetti, B. Rossi. An analytical model based on lumped parameters for the dynamic analysis of church bells. *Engineering Structures*, 32(10):3363–3376, 2010.

[17] A. B. Nordmark. Existence of periodic orbits in grazing bifurcations of impacting mechanical oscillators. *Nonlinearity*, 14(6):1517, 2001.

[18] A.B. Nordmark, P. Kowalczyk. A codimension-two scenario of sliding solutions in grazing–sliding bifurcations. *Nonlinearity*, 19(1):1, 2005.

[19] P. Brzeski, P. Perlikowski, T. Kapitaniak. Experimental verification of a hybrid dynamical model of the church bell. *International Journal of Impact Engineering* 80 177–184, 2015.

[20] P. Brzeski, P. Perlikowski, T. Kapitaniak. Analysis of transitions between different ringing schemes of the church bell. *International Journal of Impact Engineering*, 85:57–66, 2015.

[21] P. T. Piiroinen, L. N. Virgin, and A. R. Champneys. Chaos and period-adding; experimental and numerical verification of the grazing bifurcation. *Journal of Nonlinear Science*, 14(4):383–404, 2004.

[22] S. R. Bishop S. Foale. Bifurcations in impact oscillations. *Nonlinear Dynamics*, 6(3):285–299, 1994.

[23] J. M. Adam S. Ivorra, F. J. Pallares. Dynamic behaviour of a modern bell tower - a case study. *Engineering Structures*, 31(5):1085 – 1092, 2009.

[24] A. Siebert, G. Blankenhorn, K. Schweizerhof. Investigating the vibration behavior and sound of church bells considering ornaments and reliefs using ls-dyna. In *Proceedings Int. LSDYNA Conference. Detroit*, 2006.

[25] P. Thota, H. Dankowicz. Continuous and discontinuous grazing bifurcations in impacting oscillators. *Physica D: Nonlinear Phenomena*, 214(2):187–197, 2006.

[26] P. Thota, H. Dankowicz. Tc-hat (tc): a novel toolbox for the continuation of periodic trajectories in hybrid dynamical systems. *SIAM Journal on Applied Dynamical Systems*, 7(4):1283–1322, 2008.

[27] W. Veltmann. Uerber die bewgugn einer glocke. *Dinglers Polytechnisches Journal*, 220:481–494, 1876.

[28] W. Veltmann. Die koelner kaiserglocke. enthullungen uber die art und weise wie der koelner dom zu einer miï¿œrathenen glocke gekommen ist. *Hauptmann, Bonn*, 1880.

[29] H. Nusse W. Chin, E. Ott and C. Grebogi. Grazing bifurcations in impact oscillators. *Physical Review E*, 50 (6):4427, 1994.

[30] D.J. Wagg, S.R. Bishop. Chatter, sticking and chaotic impacting motion in a two-degree of freedom impact oscillator. *International Journal of Bifurcation and Chaos*, 11(01):57–71, 2001.

[31] G.S. Whiston. Global dynamics of a vibro-impacting linear oscillator. *Journal of Sound and Vibration*, 118 (3):395 – 424, 1987.

[32] S. Wiggins. *Introduction to applied nonlinear dynamical systems and chaos*, volume 2. Springer Science & Business Media, 2003.